



Penetration analysis of a projectile in ceramic composite armor

M.M. Shokrieh ^{*}, G.H. Javadpour

Composites Research Laboratory, Department of Mechanical Engineering, Iran University of Science and Technology, Narmak, 16844 Tehran, Iran

Abstract

In this research an armor material with constant thickness has been studied. The armor consists of two layers: one is a boron carbide ceramic and the other is Kevlar 49 fiber composite material. By using Ansys/Lsdyna software, the ballistic limit velocity of this armor has been obtained and the Heterington equation (optimum thickness of layers) has been verified for constant thickness of the armor. In this research, mechanical properties of Kevlar 49 under different strain rates are utilized and showed that consideration of the strain rate is very important for the simulation of penetration process. Results from the model have confirmed the validity of the Chocron–Galvez analytical model. Moreover, the projectile velocity prediction, especially at high velocity, shows a good agreement with numerical simulations. Finally, normal and oblique impacts of projectile to armor have been simulated and compared. The results show that the ballistic limit velocity of armor increases under oblique impact conditions.

© 2007 Elsevier Ltd. All rights reserved.

Keywords: Ballistic limit velocity; Ceramic composite armor; Projectile; Strain rate

1. Introduction

Traditionally, armor materials have been monolithic, usually of high hardness steel. However, the demand for lightweight armor for personal protection has led to the investigation of alternative materials. In the last few decades, non-metallic materials, such as ceramics and composites, have been increasingly incorporated into more efficient lightweight armor. In particular, due to their low density, high hardness, high rigidity and strength in compression, ceramics have become widely used in armors. Ceramic backed by composite material armor is becoming the subject of many investigations because their performance against small and medium caliber projectiles is outstanding, especially when the weight is a design condition, for instance in light weight vehicles, airplane and helicopter protection or body armor [1,2]. The main role of the ceramic material is the erosion and rupture of the projectile. However, the low fracture toughness of ceramics and, consequently, their predisposition to fracture when subjected

to high tensile stresses has led to the development of composite armors in which a ceramic-faced plate is backed by a more ductile material such as a metal or a polymeric composite that can resist failure due to tensile stresses. When armor-piercing projectiles impact onto composite armor, the projectiles are first shattered or blunted by the hard ceramic and the load is then spread over a larger area. The backing plate deforms to absorb the remaining kinetic energy of the projectile, delaying the initiation of tensile failure in the ceramic and backing plate interface, and allowing more projectile erosion [3].

Tate [4] has presented a model that is considered a basis for research in long rod penetration on thick targets. In Florence's model [5], a global energy balance is proposed leading to the derivation of the ballistic speed limit. The Woodward model [1] investigates penetration mechanism with mention of the lumped mass approach. This model presents some useful relations for calculation of velocity and residual mass of a projectile at each period of time after impact. In 1998 Chocron and Galvez [2] presented a model where the back plate of the armor is made of polymer composite material such as Kevlar/Epoxy. The model allows the calculation of residual velocity, residual mass,

^{*} Corresponding author.

E-mail address: Shokrieh@iust.ac.ir (M.M. Shokrieh).

the projectile velocity and the deflection and strain histories of the backup material. Zhu et al. [6] investigated the penetration phenomenon in Kevlar laminates due to projectile impact analytically and experimentally. Fawaz et al. [7] in their paper investigated the oblique ballistic impact on composite armor. It is shown that the projectile erosion during oblique impact is slightly greater than that of normal impact. Ballistic impact behavior of typical plain weave E-glass/epoxy and twill weave T300 carbon/epoxy composites has been studied by Naik and Shrirao [8]. A model is proposed by Ben-Dor et al. [9] for describing the penetration and perforation of monolithic FRP laminates struck transversely by a rigid projectile with an arbitrary shape. Simple relationships are given by Wen [10] to predict the penetration and perforation of monolithic fiber-reinforced plastic (FRP) laminates struck normally by projectiles with different nose shapes over a wide range of impact velocity. Thus there are many models and experiments related to composite materials under impact loading conditions presented in the literature. However, the effect of strain rate on the impact behavior of composites is not considered comprehensively.

Understanding of the material response under dynamic loading becomes imperative. This is achieved through experimental and theoretical analysis. The latter requires the development of constitutive equations, which could be used to explain the variation in material strength, stress and strain with varying strain rates. It is well-known that the yield stress of almost any material is improved with increasing strain rate. In this paper, the improved mechanical properties of Kevlar 49 due to high strain rate is presented in [11] used in simulation of impact behavior of composites.

2. Analytical methods

The design of anti-bullet armor is very complex and requires many sophisticated tools. Empirical methods are the most widely used ones because they offer reliability, but they are extremely expensive in terms of experimentation. Moreover, the results of the empirical methods do not give enough information about the history of the projectile, the trends when changing the configurations or the phenomenological process. The second way to tackle the problem is to use hydrocodes to simulate the physical process numerically. Either finite element or finite difference schemes need many parameters for material description, which very often are difficult to quantify for a correct calculation [2,9]. The numerical simulation involves finding the complete solution of some differential equations. The numerical approach provides a lot of information but again cannot give trends unless multiple configurations are calculated which consequently makes the design of armor a long and tedious process. Existing software can be used for this approach are Autodyn, Dyna3D, Lsdyna and Ansys/Lsdyna. The third approach is the analytical one. Providing the appropriate assumptions, it could be a

simple and a fast way that allows obtaining phenomenological information of the penetration mechanics without losing much accuracy with respect to the numerical models.

3. Chocron–Galvez analytical model

Chocron and Galvez [2] presented a very simple one-dimensional and fully analytical model of ballistic impact against ceramic/composite armor in their paper. Their analytical model has been checked both with ballistic tests and numerical simulations showing a good agreement. The model allows the calculation of residual velocity, residual mass, the projectile velocity and the deflection or the strain histories of the backup material. These variables are important in describing the phenomenological process of penetration. This model starts with the projectile impact on the ceramic, and then the reaction of the woven fabric and finally the combination of them represents a ceramic/composite model.

Two phases have been assumed during the impact and from that the governing equations for the projectile, ceramic plate and composite plate are considered for each of the phases and then the mathematical configuration of suggested model has been formed. The first phase is between the moment of impact to the point of ceramic cone formation, as shown in Fig. 1. When the ceramic is impacted by the projectile a compressive wave travels from the front to the rear face at the speed of sound, which is specific for each ceramic, then reflects and becomes a tensile wave which breaks the ceramic in tension. During the formation of the wave cone the projectile is being eroded but the ceramic does not move at all. The rear of the projectile moves at a velocity $v(t)$ and it is governed by Tate's equation [4]:

$$M_p \frac{dv}{dt} = -Y_p A_p. \quad (1)$$

The additional equation which governs this phase is the geometrical condition for the projectile:

$$\frac{dM_p}{dt} = -\rho_p A_p V. \quad (2)$$

The second phase starts after finishing the first phase and now the whole armor contributes to the slowing down of the projectile. As shown in Fig. 2, the rear of the projectile moves at a speed $v(t)$, the ceramic–projectile interface at $\dot{x}(t)$ and the cone at $\dot{u}(t)$. The difference between $v(t)$ and

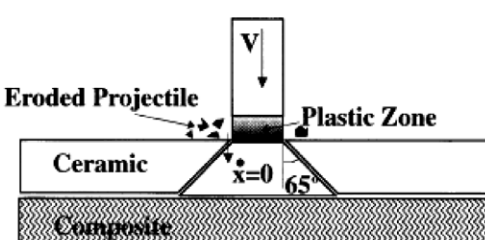


Fig. 1. Configuration at the end of the first phase [2].

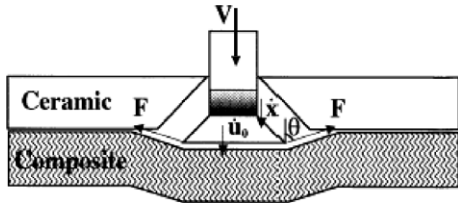


Fig. 2. Phenomenological description of the second phase [2].

$\dot{x}(t)$ gives the erosion rate of the projectile and the difference between $\dot{x}(t)$ and $\dot{u}(t)$ determines the penetration of the projectile into the ceramic cone.

3.1. Projectile equations

There is a plastic zone where the projectile is being eroded. The Alekseevskii [12] equation is applicable here:

$$Y_p + \frac{1}{2} \rho_p (V - \dot{X})^2 = Y'_c + \frac{1}{2} \rho_c (\dot{X} - \dot{U}_0), \quad (3)$$

where \dot{Y}_c is the dynamic strength of the broken ceramic. In fact the above equation shows the stress equilibrium in the ceramic-projectile interface. Deceleration of the projectile is found from Tate's equation:

$$M_p(t) \frac{dv}{dt} = -Y_p A_p. \quad (4)$$

The last equation to be written for the projectile in the first phase is the following geometrical condition:

$$\frac{dM_p}{dt} = -\rho_p A_p (V - \dot{X}). \quad (5)$$

3.2. Ceramic equations

The ceramic cone begins to move at the end of the first phase. It is pushed at one end by the projectile while, at the back, it is being retained by the composite backing layers. Fig. 3 shows the forces acting on the cone during the impact process. The equation governing the motion of the cone is Newton's equation, but now the mass is time dependent because of erosion:

$$\frac{d(M_c \dot{u}_0)}{dt} \dot{u}_0 = -2F \dot{u}_0 \cos \theta - G\pi L^2 \dot{A} + Y'_c A_p \dot{u}_0, \quad (6)$$

$$\dot{u}_0(t \equiv t_1) \equiv 0. \quad (7)$$

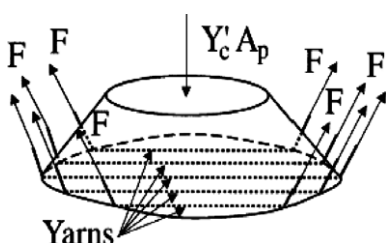


Fig. 3. Forces acting on the ceramic cone during the impact [2].

It is pointed out that Newton's equation has been multiplied by cone velocity in order to obtain an energy equation. The first and second terms in the right-hand side of the equation will be explicitly explained in the paragraph concerning the composite equations, for they are responsible for the force of the composites on the ceramic and the energy lost by delamination, respectively. The third term is the force of the projectile on the ceramic. M_c is the mass of the ceramic cone, F is the force exerted by the yarns on the ceramic cone, θ , the angle between the line of impact and the yarn, G , the energy required to delaminate 1 m^2 of composites in J/m^2 and L is a characteristic length of the backup.

3.3. Composite equations

The kinetic energy of the projectile is transmitted to the backup plate through two mechanisms: straining and breaking of the yarns, and delamination. When a point projectile impacts a linear elastic yarn the velocity $\dot{u}(t)$ of the projectile and the strain ε are related by [2]:

$$\dot{U}_0 C_y \sqrt{2\varepsilon \sqrt{\varepsilon(1+\varepsilon)} - \varepsilon^2}. \quad (8)$$

This equation is the analytical solution found by Smith et al. [13] for constant velocity impact and is also valid for a non-constant velocity provided it is only used at the point of impact as proved by Chocron et al. [14]. C_y , is the longitudinal speed of sound in the yarn and equal as $C_y = \sqrt{E/\rho}$ where E is the Young's Modulus, in high strain rate and ρ is the density of yarn. Chocron et al. [14] also found the angle between the line of impact and the yarn:

$$\sin \theta = \frac{\sqrt{2\varepsilon\sqrt{\varepsilon(1+\varepsilon)} - \varepsilon^2}}{\sqrt{\varepsilon(1+\varepsilon)}}. \quad (9)$$

The force that the yarns exert on the projectile can easily be calculated with

$$F = E \varepsilon S n_1 n_v. \quad (10)$$

The term $\pi L^2 GA$ in Eq. (6) accounts for the energy lost per unit of time due to delamination. This term is only important at low-velocity impacts, for high-velocity impacts the transversal wave has no time to progress before the failure of the panel and thus the energy absorbed by delamination is very small (less than 1% of the initial kinetic energy of the projectile) [2].

The armor that has been considered is a cubic rectangular with two layers, the front layer is boron carbide with Kevlar 49/Epoxy as the backup layer, with dimensions of the plates 40×40 mm with variable thickness. The interface of the plate consists of a kind of silicone adhesive. The relation between plates has been illustrated in modeling section. The 45° conical-cylindrical steel projectile has 30 mm length and 10 mm diameter. The mechanical properties of boron carbide are shown in Table 1 and those of the steel projectile are shown in Table 2 [7].

Table 1
Mechanical properties of boron carbide

Tangent modulus, E_t (GPa)	Yield strength, σ_y (GPa)	Stiffness, E (GPa)	Density, ρ (kg/m ³)	Poisson's ratio, ν
0	15.8	440	2500	0.17

Table 2
Mechanical properties of steel projectile [7]

Tangent modulus, E_t (GPa)	Yield strength, σ_y (GPa)	Stiffness, E (GPa)	Density, ρ (kg/m ³)	Poisson's ratio, ν
2	1069	202	7890	0.3

4. Equivalent mechanical properties of composite

In Ansys/Ls-dyna mechanical properties of composites in a normal form cannot be used, thus the equivalent mechanical properties of the laminate must be utilized. The classical lamination plate theory is used to calculate the equivalent mechanical properties of the laminate. The equivalent mechanical properties of Kevlar 49/Epoxy are shown in Table 3.

By considering the effects of strain rate on composite behavior, using Table 4 is necessary too. Wang and Xia [11] performed tensile impact experiments on Kevlar 49 fiber bundles that were carried out at various strain rates and temperatures. They found that the tensile mechanical properties of Kevlar 49 fiber bundles depend both upon the strain rate and the temperature. Table 4 lists the average properties of Kevlar 49 Fiber bundles at various strain

Table 3
Mechanical properties of Kevlar 49 composites [6]

Density, ρ (kg/m ³)	Stiffness, E (MPa)	Poisson's ratio, ν
1382	105	0.28

Table 4
Mechanical properties of Kevlar 49 fiber bundles versus strain rate and temperature [11]

	Strain rate (s^{-1})	Temperature (°C)				
		90	50	15	-20	-60
σ_{\max} (GPa)	140	2.83	2.92	2.94	2.90	2.84
	440	2.94	2.96	3.02	2.99	2.90
	1350	3.02	3.05	3.08	3.06	2.95
ε_m (%)	140	3.70	3.56	3.54	3.51	3.39
	440	3.81	3.67	3.64	3.62	3.45
	1350	3.97	3.89	3.86	3.83	3.61
E (GPa)	140	104	110	112	115	120
	440	110	116	119	120	124
	1350	115	119	125	126	129

rates and temperatures that have been used in the current numerical simulation.

5. Modeling in Ansys/Ls-dyna [15]

Because of existing the large deformation and high strain rate condition, a three-dimensional solid-64 element and the strain rate dependent plasticity material are used for modeling. Both layers of material used in the armor system are modeled with eight-node uniform hexahedron solid elements whilst the projectile is modeled with six-node tetrahedron solid elements.

The contacts occurring during impact process are: (1) contact between projectile and ceramic, (2) contact between projectile and composite, and (3) contact between ceramic and composite. The contact type that used is “eroding”. The eroding contact options are needed when the elements forming one or both exterior surfaces experience material failure during the contact. Contact is allowed to continue with the remaining interior elements. The eroding contact is used for contact between the projectile – boron carbide ceramic and the projectile – Kevlar/Epoxy composite. The “Tied” contact is used for contact between ceramic and composites. The tied contact options actually ‘glue’ the contact nodes (ceramic) to the target surfaces (composites). The effect of tied contact is that the target surfaces can deform and the slave nodes are forced to follow that deformation. When defining tied contact, the body with the coarser mesh should always be defined as the target surface [15].

Heterington [16] presented a way for calculation of optimum thickness of composite armor that is based on the energy principal. The model assumes a characteristic geometry for the fracture of the ceramic front plate and ignores the energy dissipated in fracturing the ceramic, assuming it is all delivered to the backing plate, which then is assumed to deform as a membrane. By equating the kinetic energy of the projectile to the energy absorbed in the backing plate, which deforms until it fails in tension at its ultimate tensile strain, an estimate of the ballistic limit velocity of the projectile against the armor system can be made. Finally, he found an optimum thickness ratio between the two plates of armor with using the mathematical relations as below:

$$\frac{h_1}{h_2} \approx 4 \frac{\rho_2}{\rho_1}, \quad (11)$$

where h and ρ are the thickness and density of each plate, respectively. Considering that in our model the total thickness of armor is constant at 10 mm, then:

$$h_{\text{cer}} + h_{\text{com}} = 10 \text{ mm},$$

$$\frac{h_{\text{cer}}}{h_{\text{com}}} \approx 4 \frac{\rho_{\text{com}}}{\rho_{\text{cer}}} = 4 \times \frac{1382}{2500} = 2.21.$$

Therefore, according to Heterington method [16] the optimum thickness for boron carbide and Kevlar 49/Epoxy is: $h_{\text{cer}} = 6.9$ mm and $h_{\text{comp}} = 3.1$ mm.

6. Results and discussion

As mentioned before, by having the total thickness of the armor at 10 mm, the effect of two variables, thickness ratio of the two plates and impact velocity, are investigated. The finite element model of the projectile and armor is shown in Fig. 4. Due to the axi-symmetric nature of problem, only one quarter of the projectile-armor system is modeled.

Variation of the projectile velocity versus the time is shown in Fig. 5. As shown, the projectile with 300 m/s cannot perforate the armor and after 40 s its velocity reduces to zero.

During the penetration process, the projectile is squashed and undergoes a large lateral expansion. At the

same time, the tip of the projectile is eroded as shown in Fig. 6 and the amount of eroding can be calculated from the curve shown in Fig. 5.

Variation of distance between tip and end of the projectile is shown in Fig. 7, after 40 s the amount of eroding is at a maximum and close to 7.5 mm.

The projectile residual velocities due to nine different impact projectile velocities and a comparison between the numerical and analytical solution are given in Table 5. The projectile impact velocity versus the residual velocity is shown in Fig. 8. As shown, the armor can stop the projectile with velocity up to 328 m/s and for the higher velocities the armor has been perforated.

An analytical model is obtained by writing the kinetic energy equation for the impact process and by assuming constant mass for projectile. Then the relation between impact velocity (V_s), residual velocity (V_r) and ballistic velocity (V_{50}) is obtained as below:

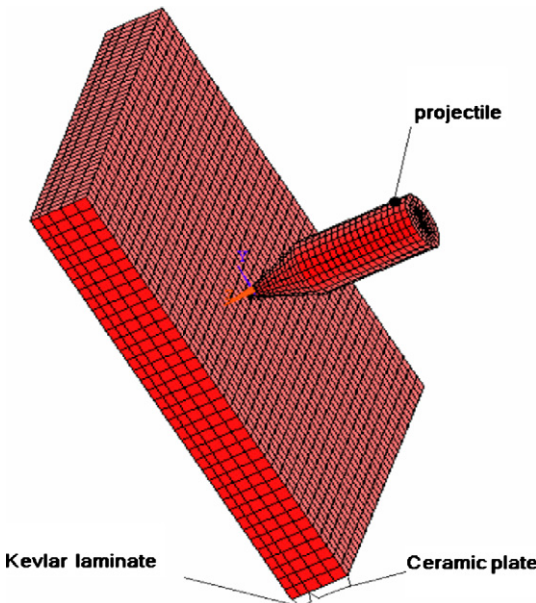


Fig. 4. Finite element model of the projectile and target.

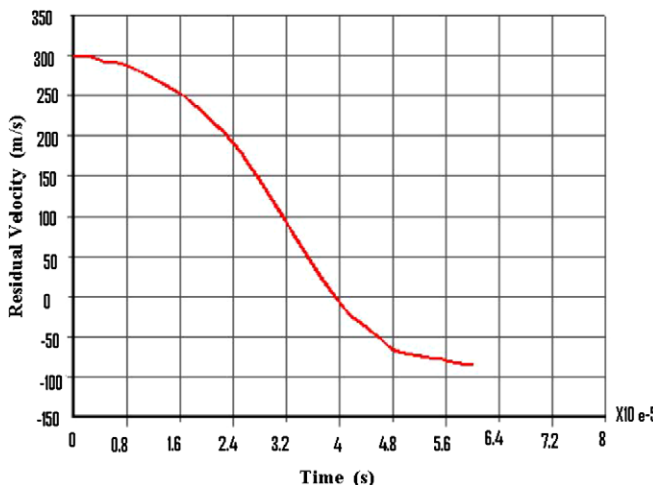


Fig. 5. Projectile residual velocity versus time; impact velocity = 300 m/s and $h_{cer} = 6.9$ mm, $h_{com} = 3.1$ mm.

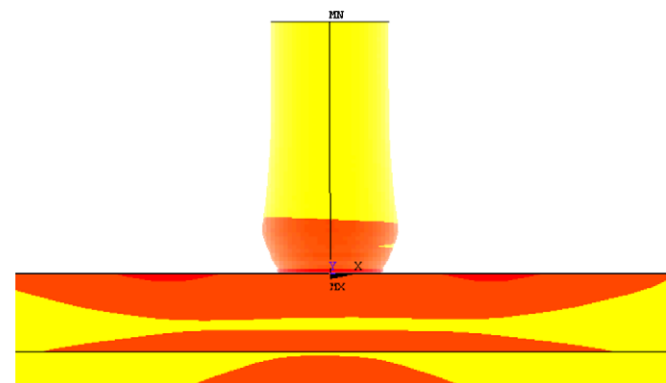


Fig. 6. Erosion of projectile with velocity 300 m/s during impact on armor with layer thickness $h_{cer} = 6.9$ mm, $h_{com} = 3.1$ mm at time 5 μ s.

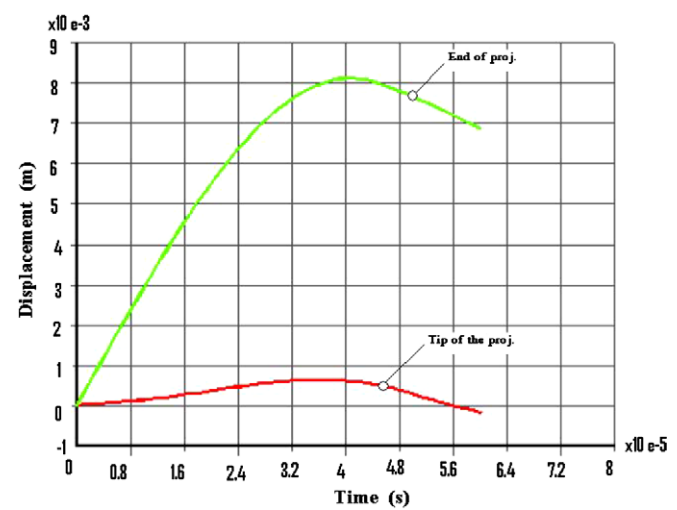
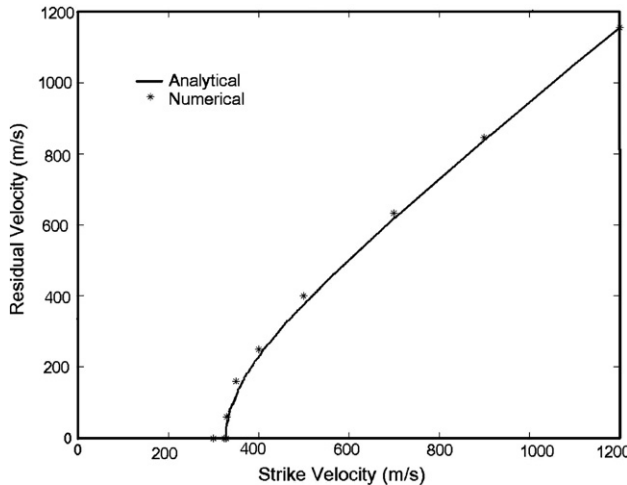


Fig. 7. Displacement variation of the tip and end of projectile with a velocity of 300 m/s during impact on an armor with layer thickness $h_{cer} = 6.9$ mm, $h_{com} = 3.1$ mm.

Table 5

Comparison of projectile residual velocity at nine different impact velocities

Strike velocity (m/s)	300	325	328	330	350	400	500	700	900	1200
Residual velocity (m/s) (numerical)	0	0	0	60	160	250	400	632	845	1155
Residual velocity (m/s) (analytical)	0	0	0	36.3	122.2	229	377.4	618.4	838.1	1154.1

Fig. 8. Projectile residual velocity versus time during impact on an armor with layer thickness $h_{cer} = 6.9$ mm, $h_{com} = 3.1$ mm.

$$\frac{1}{2}M_p V_s^2 = \frac{1}{2}M_p V_r^2 + \frac{1}{2}M_p V_{50}^2 \quad (12)$$

$$M_p = \text{const.}$$

$$V_s^2 - V_{50}^2 = V_r^2$$

By considering 328 m/s as the ballistic limit velocity, the comparison between analytical and numerical models are shown in Table 6 and Fig. 8. As it seen there is a good agreement between the analytical and numerical solutions, especially at high velocities.

The woven fabric backup armors have a specific behavior in their energy absorption. As shown in Fig. 8, when the impact velocity is 328 m/s the projectile residual velocity is zero and the projectile is stopped. But if the impact velocity increases slightly higher than the ballistic velocity, the projectile residual velocity increases more. This is the resultant of behavior of armor against impact, i.e., as the impact velocity increase up to ballistic limit the amount of absorbed energy increases, but when the impact velocity is more than the ballistic limit the capacity of absorbed energy of the system decreases drastically [16].

As shown in Fig. 8 in the high velocity cases the projectile residual velocity approaches to impact velocity and the

armor does not have any strength against the projectile as mentioned above.

7. Assessment of the model

In this section the validity of the model is assessed with the results available from the other references. It must be noted that the armor plates are similar to that mentioned in Ref. [2]. The front plate is Alumina ceramic, the composite plate is Dyneema, and the projectile is a 72 gr Tungsten projectile. With a comparison of the results from the model and those of Chocron–Galvez’s model and the other results available from Ref. [7], it is considered that there is a good agreement between them as shown in Table 6. It must be mentioned that the numerical results obtained by Chocron–Galvez are examined and evaluated by experiments [2]. Therefore, the results obtained in this research are compared with their experiments indirectly. The residual velocity of a projectile with an impact velocity of 1250 m/s versus time is shown in Fig. 9.

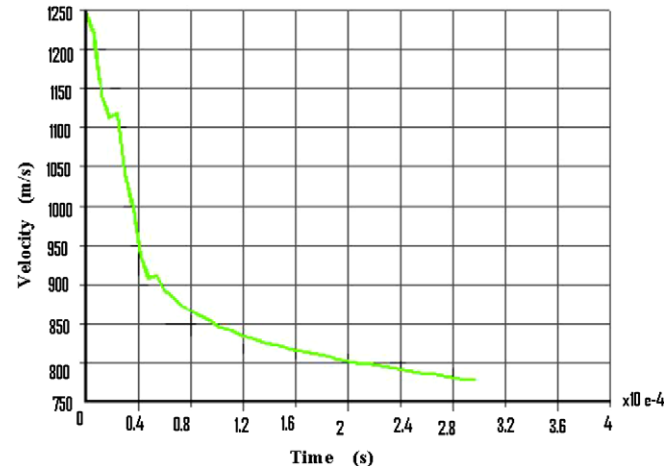
Fig. 9. Projectile residual velocity versus time; impact velocity = 300 m/s and $h_{cer} = 20$ mm, $h_{com} = 20$ mm, during impact on an armor with specifications from Ref. [12].

Table 6

Comparison of projectile residual velocity versus impact velocity during impact on an armor with specifications from Ref. [2]

Projectile residual velocity (m/s) (Autodyn)	Projectile residual velocity (m/s) (Ansys/Lsdyna)	Projectile residual velocity (m/s) (Chocron’s model)	Composite plate thickness (mm)	Ceramic plate thickness (mm)	Impact velocity (m/s)
780	770	720	20	20	1250
980	960	990	20	20	1400

8. Optimum thickness of plates

In order to calculate the optimum thickness of the ceramic and composites plates, two different thicknesses are considered. For the first case $h_{cer} = 8$ mm, $h_{com} = 2$ mm and for the second case $h_{cer} = 5$ mm, $h_{com} = 5$ mm are considered, while the optimum magnitudes of the thicknesses based on Heterington model [16] are $h_{cer} = 6.9$ mm, $h_{com} = 3.1$ mm. It must be mentioned that the total thickness of the armor is constant and equal to 10 mm. When the impact velocity is 325 m/s, in the first case, it is observed that the projectile perforates the armor and its residual velocity is 302 m/s. However, for the second case the residual velocity is 165 m/s. After investigation of the two cases along with the optimum case based on Heterington model [16], it is observed that when the ratio of the plate thicknesses is different from the optimum magnitude, the armor performance is lower than the optimum case as shown in Fig. 10.

When the thickness of ceramic is less than the optimum thickness, the boron carbide ceramic cannot stand against

the projectile and cannot erode the projectile tip. In this case the projectile perforates the armor and passes thorough it. A similar event occurs when the thickness of the ceramic is more than the optimum thickness and the thickness of Kevlar/Epoxy is less than the optimum thickness. In this case the composite layer cannot absorb the kinetic energy of the broken ceramic cone and the armor elastic properties will be sufficient.

9. Effect of oblique impact on the armor

A projectile oblique impact on the armor at a 30° angle and normal impact are compared in this section. The impact angle is an angle between the projectile axis and the normal axis of the target. As mentioned in the previous section, under the normal impact, the armor is not able to stop the projectile with a velocity more than 328 m/s.

The variation of the projectile velocity, with an impact velocity of 350 m/s and impact angle of 30° versus time is shown in Fig. 11. As shown the projectile has been stopped and it cannot perforate the armor. The results obtained from the model shows that even a projectile with an impact velocity of 400 m/s cannot perforate the armor, whilst at normal impact the armor can stop the projectile with the impact velocity of 328 m/s. The results from Ansys/LS-Dyna show that the projectile erosion in an oblique impact is greater than those of normal impact. The main reason is that the penetration path in oblique impact is longer than those for the normal impact. The results shown, as the impact angle increases the ballistic limit velocity increases too. The results presented in [7] also confirm this phenomenon.

10. Conclusion

Based on the results obtained in this research the following conclusions are summarized:

- 1 By considering the mechanical properties of composites under different strain rates, the results are more reliable.
- 2 When the impact velocity increases a small amount more than the ballistic velocity, the projectile residual velocity increases remarkably. It is due to inherent of the composites armor. As the impact velocity increases up to the ballistic limit, the amount of absorbed energy increases. However, when the impact velocity is more than the ballistic limit, the capacity of absorbed energy of the system decreases dramatically.
- 3 If the strain rate effect of the composite materials is considered, then there is a good agreement between the analytical method and numerical solution, especially at high velocities.
- 4 The Heterington equation for the optimum thickness of ceramic and composites plates of the armor is verified in this research.
- 5 The projectile erosion under oblique impacts is greater than that under normal impact. The main reason is that the penetration path under oblique impacts is longer

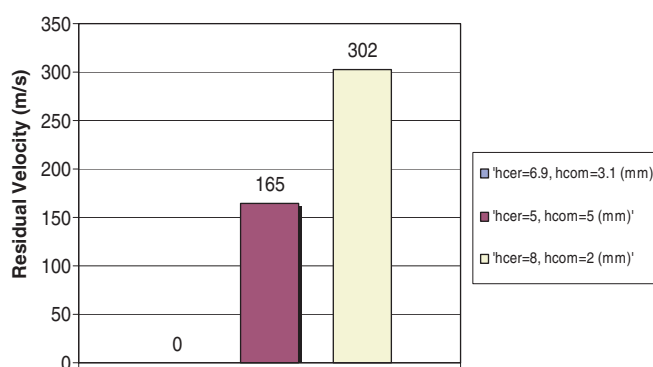


Fig. 10. Comparison curve of projectile residual velocity; impact velocity = 325 m/s, during impact on armors with difference thickness layers.

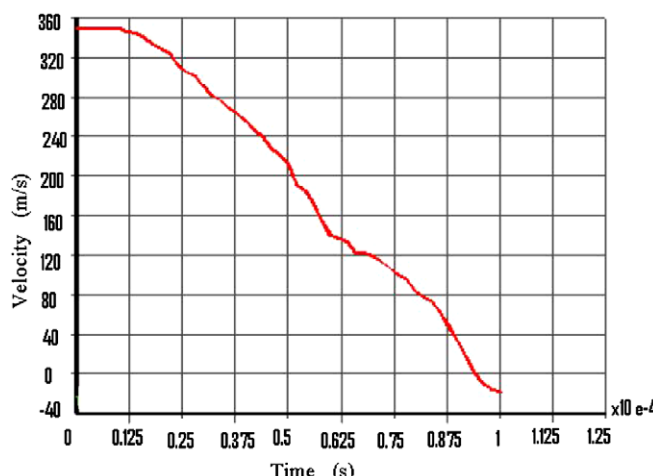


Fig. 11. Projectile velocity variation curve with oblique angle 30° and impact velocity = 350 m/s, during impact on an armor with layer thickness of $h_{cer} = 6.9$ mm, $h_{com} = 3.1$ mm.

than that under normal impacts. Also the results show, as the impact angle increases the ballistic limit velocity will also increase.

References

- [1] Woodward RL. A simple one-dimensional approach to modeling ceramic composite armor defeat. *Int J Impact Eng* 1990;9(4):455–74.
- [2] Chocron Benloulo IS, Sanchez-Galvez V. A new analytical model to simulate impact onto ceramic/composite armors. *Int J Impact Eng* 1998;21(6):461–71.
- [3] Megson THG. Aircraft structures for engineering students. Edward Arnold publishers Ltd; 1989.
- [4] Tate A. A theory for the deceleration of long rods after impact. *J Mech Phys Solids* 1967;14:387–99.
- [5] Florence AL. Interaction of projectiles and composite armor. Internal Report, US Army; August 1969.
- [6] Zhu G, Goldsmith W, Dharan CKH. Penetration of laminated Kevlar by projectiles-I. Experimental investigation. *Int J Solid Struct* 1992;29(4):399–420.
- [7] Fawaz Z, Zheng W, Behdinan K. Numerical simulation of normal and oblique ballistic impact on ceramic composite armors. *Compos Struct* 2004;63:387–95.
- [8] Naik NK, Shrira P. Composite structures under ballistic impact. *Compos Struct* 2004;66:579–90.
- [9] Ben-Dor G, Dubinsky A, Elperin T. Optimal nose geometry of the impactor against FRP aminates. *Compos Struct* 2002;55:73–80.
- [10] Wen HM. Predicting the penetration and perforation of FRP laminates struck, normally by projectiles with different nose shapes. *Compos Struct* 2000;49:321–9.
- [11] Wang Y, Xia YM. Experimental and theoretical study on the strain rate and temperature dependence of mechanical behavior of Kevlar fiber. *Compos Part A* 1999;30(11):1251–7. November.
- [12] Alekseevskii VP. Penetration of a rod into a target at high velocity. Combustion explosion and shock waves, vol. 2. New York, USA: Faraday Press; 1966.
- [13] Smith JC, McCrackin FL, Schiefer HF. Stress-strain relationships in yarns subjected to rapid impact loading, Part V: wave propagation in long textile yarns impacted transversely. *Textile Res J* 1958:288–302.
- [14] Chocron Benloulo IS, Rodryguez J, Sanchez Galvez V. A simple analytical model to simulate textile fabric ballistic impact behavior. *Textile Res J Tentative* 1997(July).
- [15] Ansys/Ls-Dyna. User's manual, nonlinear dynamic analysis of structures in three dimensions.
- [16] Hetherington JG. The optimization of two-component composite armors. *Int J Impact Eng* 1992;12:229–59.